Supporting Information

The Malaria Pigment Hemozoin Comprises at Most Four Different Isomer Units in Two Crystalline Models: Chiral as Based on a Biochemical Hypothesis, or Centrosymmetric Made of Enantiomorphous Sectors

Tine Straasø[1]*, Noa Marom[2*], Inna Solomonov[3], Lea K. Barfod[4,5], Manfred Burghammer[6], Robert Feidenhans'l[1], Jens Als-Nielsen[1]*, Leslie Leiserowitz[7]*

[1]Niels Bohr Institute, University of Copenhagen, 2100 Copenhagen, Denmark, [2]Department of Physics and Engineering Physics, Tulane University, New Orleans, LA 70118, USA, [3]Department of Biological Regulation, The Weizmann Institute of Science, 76100-Rehovot, Israel, [4]Center for Medical Parasitology, Department of International Health, Immunology and Microbiology, University of Copenhagen, 2200 Copenhagen, Denmark, [5]Department of Infectious Diseases, Copenhagen University Hospital (Rigshospitalet), 2100 Copenhagen, Denmark, [6]European Synchrotron Radiation Facility, 38043 Grenoble, France, [7]Department of Materials and Interfaces, The Weizmann Institute of Science, 76100-Rehovot, Israel.

Figure S1 Schematic representation of the formation of the four different stereoisomers of Fe-O cyclic Fe(3+) PPIX dimers, attributable to the enantio-facial symmetry of the monomer molecules from which they are assembled. The porphyrin ring is depicted as a line, when viewed along the axis indicated by the two 'eyes' (I and II) in the insert. Pyrrole rings A and B are represented by a diamond, and rings C and D are represented by a square. The direction of the propionic acid groups viewed from eye I is represented by a cross, while from eye II, it is represented by a circle. (a) The monomer as viewed from eye II. (b) Two Fe(3+) PPIX monomers, related to each other by a center of inversion ($\bar{1}$), are positioned directly above one another, prior to reciprocal Fe-O coordination. (c) With prior appropriate deprotonation ($C_2H_4CO_2^-$, light red signature) of one of the two acid groups ($C_2H_4CO_2H$, designated by dark red) of each monomer, Fe-O coordination can come about by a relative shift of the monomers as indicated by arrows. Two centrosymmetric Fe-O cyclic dimer isomers may be formed, labeled $cd\bar{1}_1$ and $cd\bar{1}_2$. The rotation of 180° of $cd\bar{1}_2$ is for convenient comparison with $cd\bar{1}_1$. (d) Two Fe(3+) PPIX monomers, related to each other by twofold (2) symmetry prior to Fe-O coordination. (e) Upon binding, two chiral cyclic dimers of opposite handedness may form. We

arbitrarily denote their chirality by (-) and (+) signs and the dimers by the symbols *cd*2(-) and *cd*2(+). Reprinted with permission from Straasø *et al.*, *Crystal Growth & Des.* **2011**, *11*, 3342. Copyright 2011 American Chemical Society.

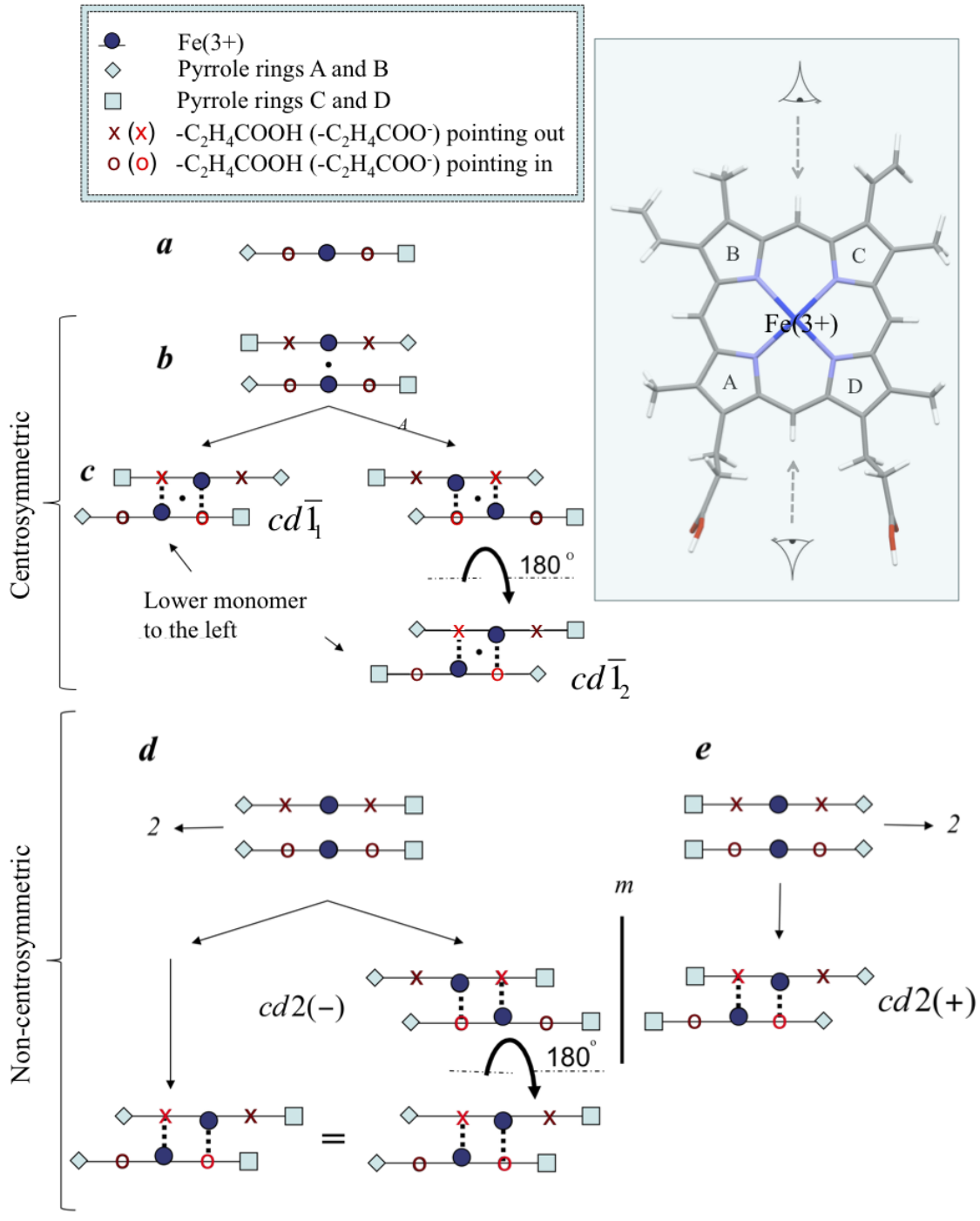

Figure S2 The heme-O_2 complex in myoglobin[2] shows the same orientational ordering as in hemoglobin. Molecular oxygen is bound to the *Re* face of the heme, while histidine is bound to the opposite *Si* face. The color code from Scheme 1 has been applied for easy comparison. The structure is generated from the pdb file published by Ref. 2.

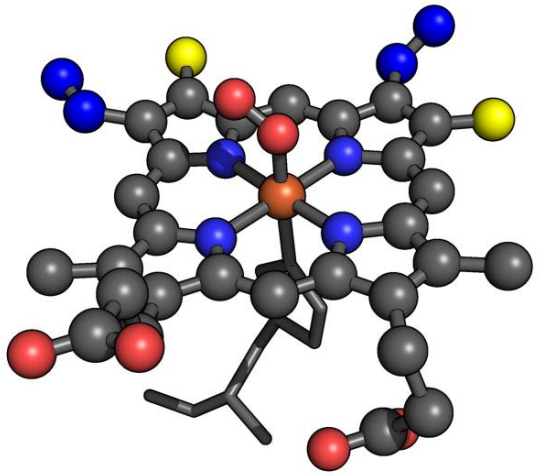

Structural information of the refined structure (calculated for one monomer):

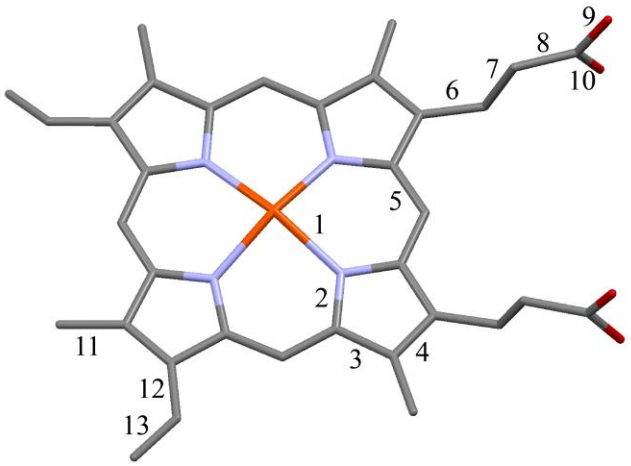

Table S1: Averaged lengths of chemically equivalent (eq.) bonds of the heme moiety in the refined crystal structure of hemozoin.

No. (see scheme)	Bond type	No. of eq. bonds	Bond length (Å)
-	OH···O(=C)	1	2.70
-	Fe-O (not shown)	1	1.89
1	Fe-N	4	2.082(3)
2	N-C	8	1.3762(6)
3	C-C (pyrrole)	8	1.446(2)
4	C-C (pyr.)	4	1.3828(0)
5	C(pyr.)-C(H)	8	1.393(2)
6	C(pyr.)-C_β(prop.)	2	1.501(1)
7	$C_\beta(H_2)$-$C_\alpha(H_2)$	2	1.528(4)
8	$C_\alpha(H_2)$-$C(O_2)$	2	1.503(1)
9	C=O	2	1.225(7)
10	C-O(Fe or H)	2	1.326(7)
11	C-C (methyl)	4	1.490(1)
12	C-C (vinyl)	2	1.4505(1)
13	C=C (vinyl)	2	1.335(8)

Table S2. Structural parameters (in Å, degrees) and binding energies (BE, kcal/mol) with respect to two heme monomers and a hydrogen molecule calculated with PBE+TS for isolated dimers in the intermediate (J=7) and high (J=11) spin states. The interplanar distance is calculated for the porphyrin cores of the two monomers, excluding all the side groups and the Fe atoms. If the porphyrin cores are not parallel to each other the interplanar distances is approximate. The calculated structural parameters are compared to the refined structures from XRPD.

In the isolated dimers, the Fe-Fe distances and the C-C-C-C torsion angles on the propionate bridges are smaller than in the β-hematin and hemozoin crystals. This indicates a greater overlap between the π-systems of the heme monomers in the isolated dimers than in the β-hematin and hemozoin crystals. The *cd2*(+) dimer gains stabilization from binding two O_2 molecules, which means that the *cd2*(+)+2O_2 complex is feasible. In this complex the Fe atom remains close to the porphyrin plane and the Fe-O_2 bond length of 1.93 Å is larger than the bond length of 1.77 Å in the heme+O_2 complex and of 1.73 Å in the heme+O_2+H_2O complex.

	cd*$\bar{1}_1$		***cd*$\bar{1}_2$***		***cd*2(+)**		***cd2*(+)+2O_2**	**β-hematin****		**hemozoin**†
J	**7**	**11**	**7**	**11**	**7**	**11**	**3**	**major**	**minor**	
BE w/r to 2*heme - H_2	-24.76	-4.34	-20.57	-1.99	-21.57	-2.59	-17.20***			
Interplanar distance	4.82	4.91	5.17	5.03	~4.63	~4.58	~5.09	4.59	4.57	4.55
Mean deviation from planarity	0.12	0.11	0.12	0.08	0.08 0.06	0.06 0.03	0.04 0.11	0.03	0.03	0.03
Fe shift from porphyrin plane	0.27	0.48	0.23	0.44	0.24 0.26	0.46 0.48	0.02 0.04	0.49	0.46	0.47
Fe-Fe distance	7.03	6.81	8.63	8.53	8.69	8.60	8.77	8.94	9.24	9.03
C-C-C-C torsion angle on propionate bridge	86.6	85.9	176.6	175.1	179.9 93.3	177.1 98.2	175.4 167.6	174.6	172.8	168.3 168.1
C-C-C-C torsion angle on propionic acid	176.9	177.2	175.6	173.9	178.4 178.6	177.6 179.3	179.0 170.9	166.7	162.8	169.6 171.3

* Data from Marom *et al.*[3]

** Data from Straasø *et al.*[1]

*** BE with respect to a *cd2*(+) dimer and two O_2 molecules

† Based on the refined structure of the *cd2*(+) dimer in the unit cell of hemozoin

Table S3. Structural parameters (in Å, degrees) calculated with PBE+TS for heme dimers in the intermediate (J=7) and high (J=11) spin states *in the unit cell of the major phase of β-hematin*. The interplanar distance is calculated for the porphyrin cores of the two monomers, excluding all the side groups and the Fe atoms. If the porphyrin cores are not parallel to each other the interplanar distance is approximate. The calculated structural parameters are compared to the refined structure from XRPD.

	cd*$\bar{1}_1$		***cd*$\bar{1}_2$***		***cd*2(+)**		**XRPD****
J	**7**	**11**	**7**	**11**	**7**	**11**	
Interplanar distance	4.62	4.66	~4.46	~4.54	~4.51	~4.53	4.59
Mean deviation from planarity	0.02	0.03	0.05 0.06	0.06	0.04	0.04 0.05	0.03
Fe shift from porphyrin plane	0.29	0.49	0.26 0.24	0.48 0.46	0.30 0.31	0.49 0.52	0.49
Fe-Fe distance	9.12	9.04	8.95	8.87	9.19	9.11	8.94
C-C-C-C torsion angle on propionate bridge	172.1	174.6	175.1 170.3	177.0 172.7	166.5 165.1	169.1 167.7	174.6
C-C-C-C torsion angle on propionic acid	166.0	166.7	170.7 164.4	172.0 165.6	165.6 168.1	166.5 168.8	166.7
H-bond O···O distance	2.65	2.66	2.68 2.63	2.68 2.66	2.63 2.62	2.64 2.63	2.70

* Data from Marom *et al.*[3] We note that the non-centrosymmetric dimer reported therein was the *cd2*(-) dimer.

** Data from Straasø *et al.*[1]

Table S4. Structural parameters (in Å, degrees) calculated with PBE+TS for heme dimers in the intermediate (J=7) and high (J=11) spin states *in the unit cell of the minor phase of β-hematin*. The interplanar distance is calculated for the porphyrin cores of the two monomers, excluding all the side groups and the Fe atoms. If the porphyrin cores are not parallel to each other the interplanar distance is approximate. The calculated structural parameters are compared to the refined structure from XRPD.

	$cd\bar{1}_1$*		$cd\bar{1}_2$*		*cd*2(+)		XRPD**
J	**7**	**11**	**7**	**11**	**7**	**11**	
Interplanar distance	4.49	4.54	4.35	4.42	~4.37	~4.42	4.57
Mean deviation from planarity	0.02	0.02	0.03	0.02	0.03 0.02	0.02	0.03
Fe shift from porphyrin plane	0.27	0.46	0.27	0.45	0.27	0.46	0.46
Fe-Fe distance	9.35	9.34	9.37	9.33	9.28	9.27	9.24
C-C-C-C torsion angle on propionate bridge	166.6	165.5	160.3	161.3	166.7 164.2	167.8 165.2	172.8
C-C-C-C torsion angle on propionic acid	167.0	168.8	168.4	169.3	163.4 167.6	164.9 168.0	162.8
H-bond O···O distance	2.64	2.65	2.62	2.63	2.64 2.63	2.66 2.64	2.65

* Data from Marom *et al.*[3] We note that the non-centrosymmetric dimer reported therein was the *cd2*(-) dimer.

** Data from Straasø *et al.*[1]

Table S5. Structural parameters (in Å, degrees) calculated with PBE+TS for heme dimers in the intermediate (J=7) and high (J=11) spin states *in the unit cell of hemozoin*. The interplanar distance is calculated for the porphyrin cores of the two monomers, excluding all the side groups and the Fe atoms. If the porphyrin cores are not parallel to each other the interplanar distance is approximate. The calculated structural parameters are compared to the refined structure from XRPD.

	***cd*$\bar{1}_1$**		***cd*$\bar{1}_2$**		***cd*2(+)**		**XRPD†**
J	**7**	**11**	**7**	**11**	**7**	**11**	
Interplanar distance	4.75	4.81	~4.66	~4.69	~4.58	~4.61	4.55
Mean deviation from planarity	0.03	0.03	0.05 0.06	0.06	0.05 0.04	0.05	0.03
Fe shift from porphyrin plane	0.29	0.49	0.28 0.27	0.47 0.48	0.30 0.31	0.50 0.52	0.47
Fe-Fe distance	9.18	9.11	8.95	8.86	9.21	9.14	9.03
C-C-C-C torsion angle on propionate bridge	167.8	170.2	174.7 173.2	176.7 174.6	166.6 164.9	168.6 167.3	168.3 168.1
C-C-C-C torsion angle on propionic acid	167.1	167.5	165.9 168.3	166.6 169.7	165.7 168.3	166.7 168.8	169.6 171.3
H-bond O···O distance	2.65	2.66	2.70 2.68	2.71 2.68	2.64 2.63	2.66 2.65	2.67 2.69

† Based on the refined structure of the *cd2*(+) dimer in the unit cell of hemozoin

Table S6. Binding energy per unit cell with respect to two heme monomers and a hydrogen molecule and lattice energy per unit cell with respect to a heme dimer in the same spin state (kcal/mol), calculated with PBE+TS for heme dimers in the intermediate (J=7) and high (J=11) spin states in the unit cells of the two phases of β-hematin and of hemozoin.

The $cd\bar{1}_1$ isomer is less stable in the unit cells of the minor phase of β-hematin and of hemozoin than in the unit cell of the major phase of β-hematin. The $cd\bar{1}_2$ isomer is less stable in the unit cell of the major phase of β-hematin than in the unit cells of the minor phase of β-hematin and of hemozoin. The *cd2*(+) isomer is the less stable in the unit cell of the minor phase of β-hematin than in the unit cells of the major phase of β-hematin and of hemozoin. These results are consistent with the major phase of β-hematin comprising $cd\bar{1}_1$ and *cd2*(+) dimers, the minor phase of β-hematin comprising the $cd\bar{1}_2$ isomer, and hemozoin comprising a mixture of isomers. We note that the unit cell parameters were not fully relaxed and the effects of temperature and of isomeric disorder were not taken into account.

		$cd\bar{1}_1$		$cd\bar{1}_2$		*cd2*(+)	
J		**7**	**11**	**7**	**11**	**7**	**11**
β-hematin (major)	BE	-171.10*	-151.53*	-154.33*	-135.53*	-165.95	-146.47
	E_{latt}	-146.34*	-147.19*	-133.76*	-133.54*	-144.38	-143.88
β-hematin (minor)	BE	-160.88*	-141.85*	-156.94*	-136.00*	-153.95	-134.65
	E_{latt}	-136.12*	-137.50*	-136.37*	-134.01*	-132.38	-132.07
Hemozoin	BE	-168.15	-149.54	-158.40	-137.40	-164.43	-145.48
	E_{latt}	-143.39	-145.19	-137.84	-135.41	-142.86	-142.90

* Data from Marom *et al.*[3] We note that the non-centrosymmetric dimer reported therein was the *cd2*(-) dimer.

Enantioselective occlusion of hematin anhydride and chiral symmetry of hemozoin. Assuming the crystal structure of hemozoin is basically centrosymmetric, composed of $cd\bar{1}_1$ dimers, its {*h,k,l*} crystal faces are therefore chiral, exposing enantiotopic (*h,k,l*) and ($\bar{h},\bar{k},\bar{l}$) surfaces. Basing ourselves on an analysis of intermolecular contacts, we had previously shown (see Fig. 7 in Ref. 1) that the *cd*2(±) dimers can, without impediment, be enantioselectively adsorbed onto the {010}, {011}, and {100} crystal faces, the latter less easily though, and be eventually occluded within the growing crystal; cd2(+) can bind to the $(0\bar{1}0)$ (011), and $(\bar{1}00)$ faces, cd2(-) can bind to the (010), $(0\bar{1}\bar{1})$, and (100) faces. The centrosymmetric $cd\bar{1}_2$ isomer cannot easily be adsorbed onto any of the regular crystal faces. Thus different sectors of the crystal may be chiral of opposite handedness, but an X-ray diffraction refinement of the whole crystal will yield a disordered centrosymmetric crystal structure composed of both $cd\bar{1}_1$ and $cd\bar{1}_2$ dimers, since a 1:1 mixture of cd2(+) and cd2(-) enatiomers, even in different sectors of the submicron-sized crystals, will be diffractionally essentially equivalent to a disordered mixture of $cd\bar{1}_1$ and $cd\bar{1}_2$ dimers.

Many different studies, however, point towards an oriented, lipid-templated nucleation of the crystal[4-12] occurring from its {100} face both in β-hematin[8,9] and hemozoin,[11,12] which, in the latter, occurs via the inner membrane surface of the parasitic digestive vacuole in the infected red blood cell. Thus hemozoin nucleated via its (100) face, will expose to the hematin anhydride molecules in the aqueous environment of the digestive vacuole the opposite $(\bar{1}00)$ face which may preferentially bind *cd*2(+) dimers rather than the opposite enantiomer. Given that hematin anhydride will be occluded at the nucleation stage into the growing crystal via all its faces but for the $(\bar{1}00)$, and the observation that hemozoin crystals are detached from the membrane wall at some point after nucleation, the proposed chiral symmetry of hemozoin cannot be due to preferential occlusion of one of the two hematin anhydride enantiomers.

.

Determination of absolute structure of the chiral hematin anhydride dimer in a hemozoin crystal of proposed chiral symmetry. To determine the absolute structure of a single crystal (of hemozoin), the atoms inducing molecular handedness cannot all be of the same element and

should preferably exhibit strong anomalous scattering at a suitable wavelength. Thus the chirality of the cd2(+) dimer, which arises basically from the pseudo twofold symmetry relating four vinyl and four methyl substituents at eight atomic sites on pyrrole rings *B* and *C* of two heme molecules would not be evident in terms of X-ray diffraction. Thus, we assigned the handedness of the hematin anhydride dimer cd2(+) based on our model for the hematin anhydride dimer formation, where the *Si* sides of the two heme molecules would be free to coordinate whereas the opposite *Re* sides would be bound to O_2 as in hemoglobin (see main text).

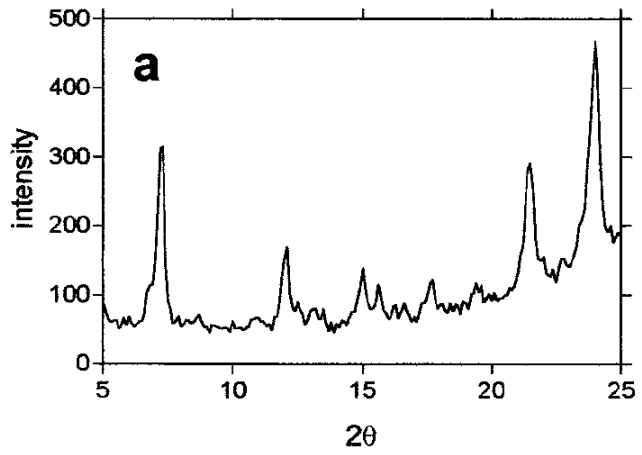

Fig. S3a. Reprint of Fig. 3a by Egan *et al.*[13] The {100} reflection, 2θ ≅ 7°, of wet β-hematin exhibits a pro-nounced shoulder indicative of the presence of the minor phase. Reprinted with permission from Egan *et al.*, *Biochemistry-Us* **2001**, *40*, 204. Copyright 2001 American Chem. Soc.

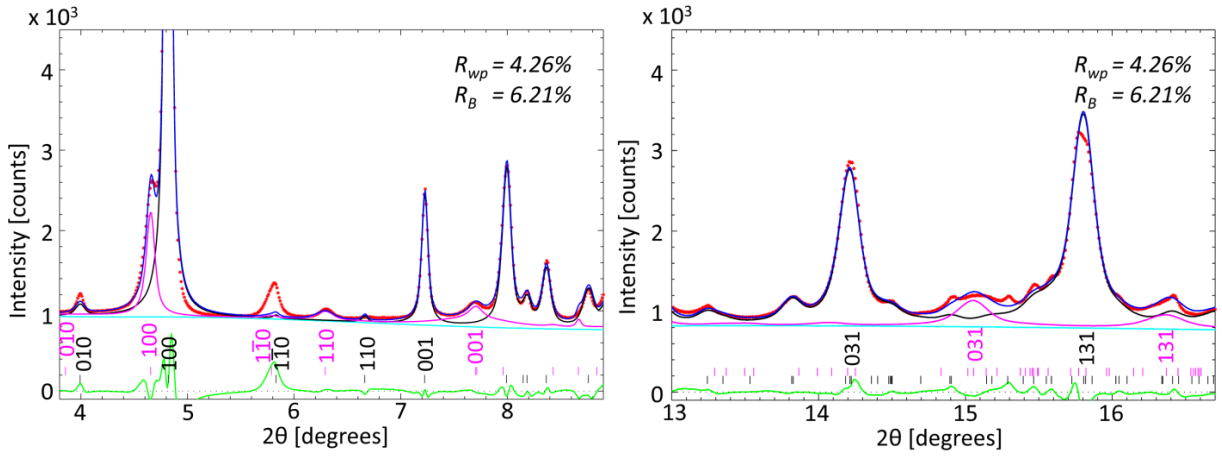

Figure S3b. Reprint of Figure 8 in Ref. 1. The reflections from the minor phase are shown in magenta. Explicitly the 100, 110, 001, 031 and 131 reflections are resolvable.

Table S7. The H-bonding axial length and unit cell volume in several β-hematin (βH) and hemozoin (Hz) crystals

Hemozoin and β-hematin at a temp. of 300 K	***a*-*c*** (Å)	V ($Å^{-3}$)
βH[a]	15.38	1416
βH[b]	15.40	1423
βH[c]	15.36	1411
βH[d]	15.40	1414
Hz[c] *S. mansoni*	15.42	1427
Hz[c] *R. prolixus*	15.36	1425
Hz[e] *P. falciparum*	15.40	1423

Hemozoin and β-hematin at temp. of 50-90 K	***a*-*c*** (Å)	V ($Å^{-3}$)
βH[b] (50 K)	15.26	1384
βH[d] (90 K)	15.26	1375
Hz[e] *P. falciparum* (80 K)	15.29	1391
Hz[f] *P. falciparum* (80 K)	15.39	1416

[a]Pagola *et al.*[14], [b]Bohle *et al.*[15], [c]Oliviera *et al.*[16], [d]Straasø *et al.*[1] Note that the unit cell dimensions of the crystals at 300 K had not been published. [e]Present study. [f]Klonis *et al.*[17] The unit cell volume of the crystal structure reported by Klonis *et al*. suggests that the crystal temperature was closer to room temperature than the reported 80 K.

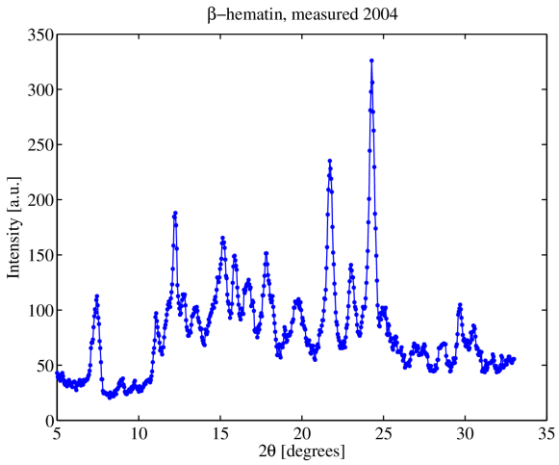

Figure S4: The raw PXRD data of a β-hematin sample measured on an in-house set-up in 2004. Due to the experimental set-up, the intensity of the {100} reflection at 2θ ~ 7° is heavily reduced.

The repeated formation of significant quantities of the minor phase of β-hematin from different crystallization batches rules out the possibility of an impurity phase, but rather points to the fact that the minor phase is a product of the reacting agents which in this case were 98% pure chloro-hemin, dry MeOH and 2.6-lutidine (added in excess). In the hypothetical case that a fraction of the original chloro-hemin phase remained unreacted was ruled out by a comparison of the calculated XRPD pattern of chloro-hemin and the observed reflections of the minor phase of β-hematin . Moreover the FTIR spectra showed the characteristic strong and narrow bands at 1206 and 1660 cm^{-1}, indicative of the iron-coordinated C-O and C=O stretching vibrations, which are absent in chloro-hemin.

Table S8 Selected *d*-spacings (Å) of the two different β-hematin samples measured by means of nano-diffraction (ESRF) and XRPD, respectively.

Reflection	ESRF	2004 XRPD measurement
$\{100\}_{major}$	12.00	11.94
$\{100\}_{minor}$	12.39	12.42
$\{020\}_{major}$	7.25	7.22
$\{020\}_{minor}$	7.47	7.49
$\{031\}_{major}$	4.10	4.08
$\{031\}_{minor}$	3.87	3.70
$\{131\}_{major}$	3.68	3.66
$\{131\}_{minor}$	3.58	3.55

Table S9. Binding energy (in kcal/mol), spin state, and some structural parameters (bond lengths in Å and angles in degrees) of different configurations of a five-coordinated heme+O_2 complex, illustrated in Figure S4. All the structures were fully relaxed with spin unrestricted PBE+TS. The binding energy is insensitive to rotation of the oxygen molecule on top of the heme. The O-O bond in the bound molecule is slightly longer than in the free molecule (1.27 vs. 1.21 Å).

Configuration	J	Binding Energy	Fe-O	O-O	Fe-O-O
a	1	24.39	1.765	1.27	121.89
b	1	24.42	1.765	1.27	121.85
c	1	24.39	1.766	1.27	121.86
d	1	24.37	1.765	1.27	121.82

Figure S5. Configurations of a five-coordinated heme+O_2 complex

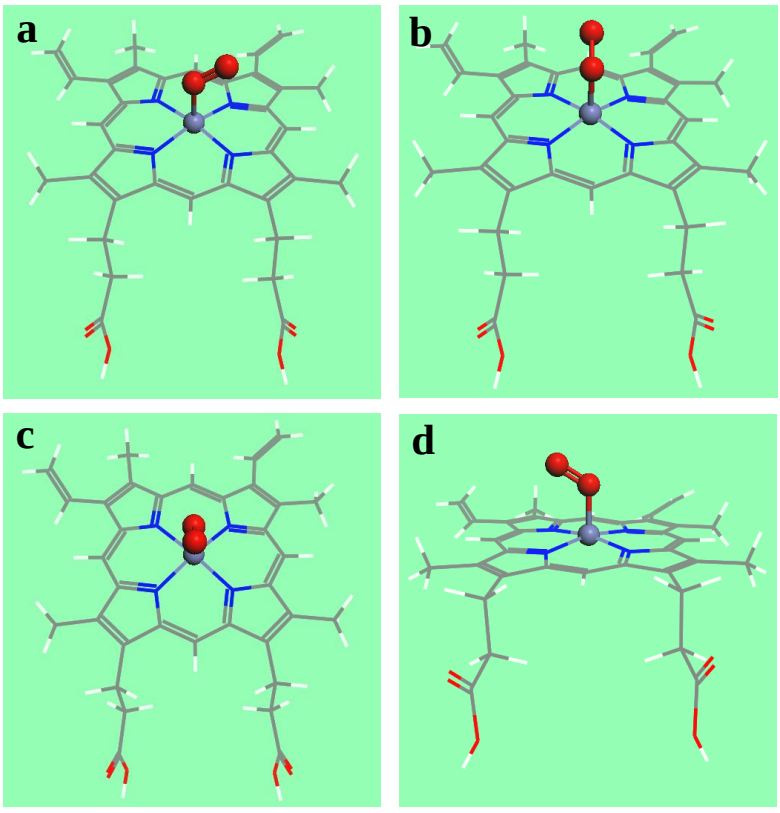

Table S10. Binding energy (in kcal/mol), spin state, and some structural parameters (bond lengths in Å and angles in degrees) of different configurations of a six-coordinated imidazole+heme+O_2 complex, illustrated in Figure S5. All the structures were fully relaxed with spin unrestricted PBE+TS. The binding energy is insensitive to rotation of the imidazole and the oxygen molecule with respect to the heme. The O-O bond in the bound molecule is slightly longer than in the free molecule (1.27 vs. 1.21 Å). The binding energy of the six-coordinated complex is lower than that of the five-coordinated complex.

Configuration	J	Binding Energy	Fe-O	O-O	Fe-O-O
a-a	1	20.25	1.755	1.274	122.21
a-b	1	20.24	1.755	1.274	122.48
a-c	1	20.27	1.755	1.274	122.35
a-d	1	20.24	1.755	1.274	122.42
b-a	1	20.31	1.755	1.274	122.42
b-b	1	20.26	1.755	1.274	122.22
b-c	1	20.26	1.755	1.274	122.60
b-d	1	20.27	1.755	1.274	122.33

Figure S6. Configurations of a six-coordinated imidazole+heme+O_2 complex

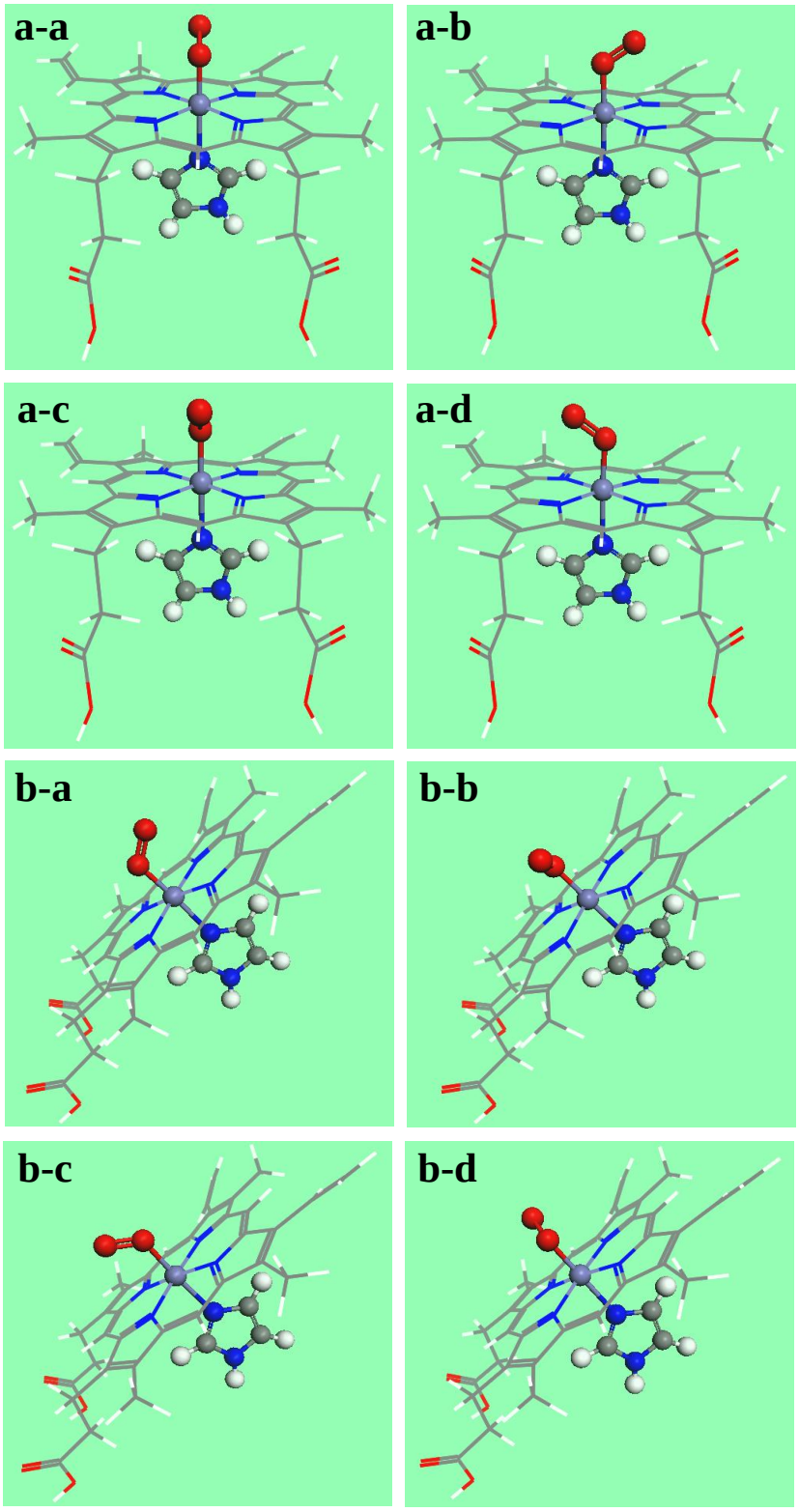

Table S11. Binding energy (in kcal/mol), spin state, and some structural parameters (bond lengths in Å and angles in degrees) of different configurations of a five-coordinated heme+H_2O complex, illustrated in Figure S6. All the structures were fully relaxed with spin unrestricted PBE+TS. The binding energy is largely insensitive to rotation of the water molecule with respect to the heme. However, the binding is somewhat stronger on the *Re* side than on the *Si* side. The heme-H_2O interaction is weak and predominantly dispersive. The geometry of the bound water molecule is almost identical to the free molecule.

Side	Configuration	J	Binding Energy	Fe-O	O-H	H-O-H	Fe-O-H
Re	a	1	-0.97	1.980	0.977	105.18	101.95/101.73
	b	1	-0.92	1.980	0.977	105.23	101.58/102.22
	c	1	-1.01	1.980	0.977	105.15	101.40/101.80
	d	1	-1.06	1.980	0.977	105.16	101.75/101.77
Si	e	1	-0.66	1.982	0.977	105.15	101.45/101.58
	f	1	-0.51	1.982	0.977	105.08	100.32/102.19
	g	1	-0.33	1.981	0.977	105.13	100.93/101.28
	h	1	-0.43	1.981	0.977	105.12	100.71/101.93

Figure S7. Configurations of a five-coordinated heme+H_2O complex

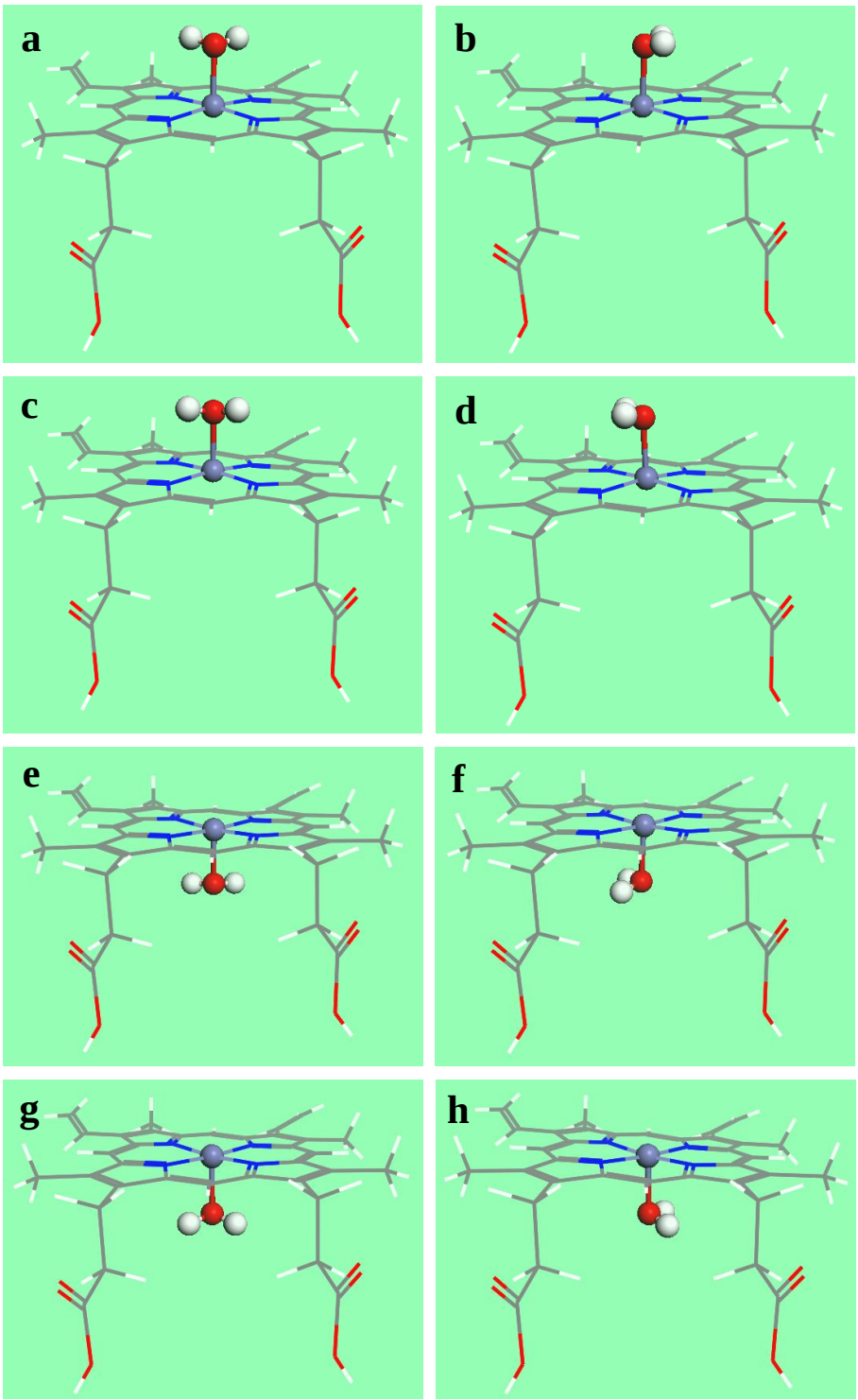

Table S12. Binding energy (in kcal/mol), spin state, and some structural parameters (bond lengths in Å and angles in degrees) of different configurations of a six-coordinated O_2+heme+H_2O complex, illustrated in Figure S7. The oxygen is bound on the *Re* side and the water is bound on the *Si* side. All the structures were fully relaxed with spin unrestricted PBE+TS. The binding energy is largely insensitive to rotation of the oxygen and water molecules with respect to the heme. The binding energy of this complex is significantly higher than that of a five-coordinated heme+O_2 complex. As in the five-coordinated heme+O_2 and heme+H_2O complexes, the O-O bond in the bound molecule is slightly longer than in the free molecule (1.27 vs. 1.21 Å) and the geometry of the bound water molecule is almost identical to the free molecule.

Configuration	J	Binding energy	Fe-O (O_2)	O-O	Fe-O-O	Fe-O (H_2O)	O-H	H-O-H	Fe-O-H
A	1	-32.90	1.731	1.272	122.36	2.273	0.974	104.19	95.88
B	1	-32.87	1.731	1.272	122.14	2.284	0.974	104.25	96.49

Figure S8. Configurations of a six-coordinated O_2+heme+H_2O complex

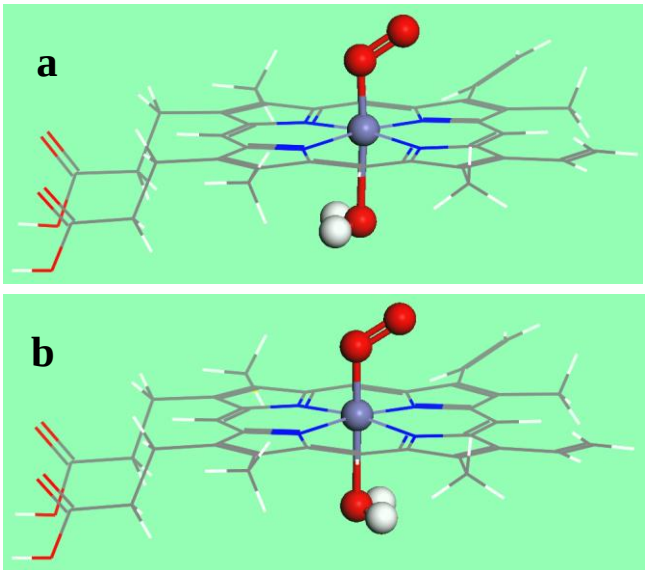

Figure S9. The relaxed structure of a complex of a *cd2*(+) dimer with two oxygen molecules bound on the *Re* side of the heme iron (H atoms are not shown). Such a complex may form if oxygen remains bound to the heme when it is cleaved from the globin by the malaria parasite. This may lead to hemozoin comprising *cd2*(+) dimers preferentially.

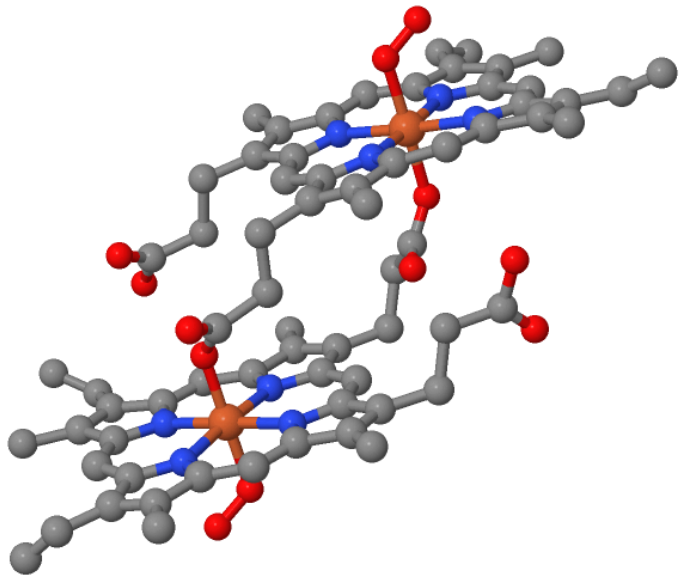

Figure S10. It is not possible to form a H-bonded ‘chain’ from the hematin anhydride dimers via twofold symmetry, since it would lead to sterically bad contacts, compared to interlinkage via inversion symmetry.

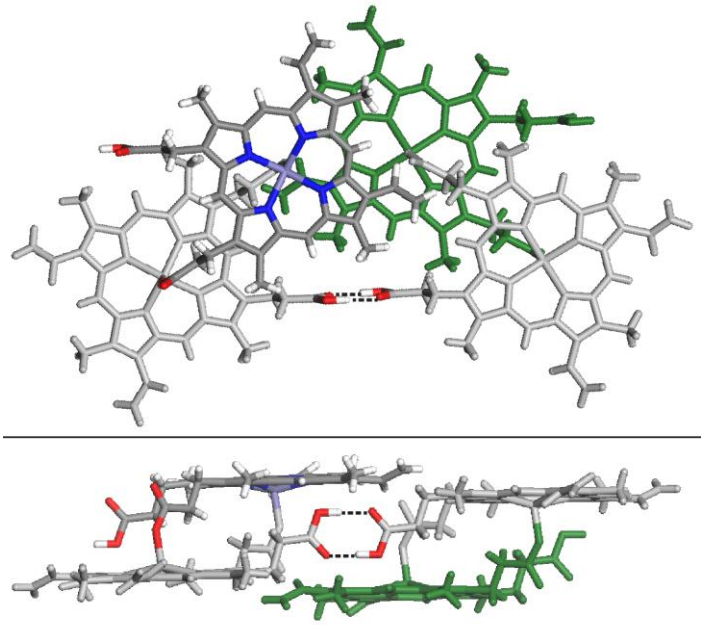

Figure S11. C-H···O (carboxylate) bonds forming the bilayer. The H-bonded hematin anhydride chains (Fig. 7a,b) mesh so as to form both C-H···O contacts of 2.8-2.9 Å between ethylene proton donors and the exposed lone pair electron lobes of the two propionate O atoms (as depicted here in the figure) and π-π contacts between *c*-translation related hematin anhydride dimers (as also shown in Fig. 7c,d).

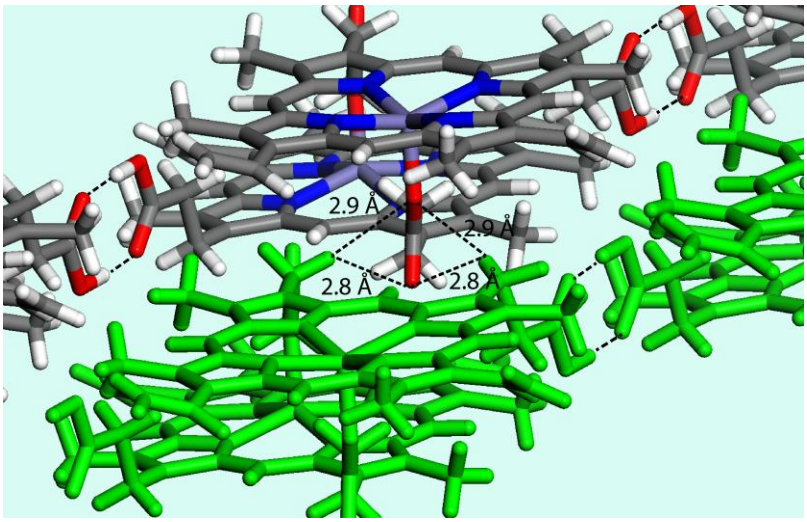

Table S13. Fe-Fe distances (Å) within (i.e. *intra*) and between (i.e., *inter*) hematin anhydride dimers in the crystal structures of hemozoin (Hz), β-hematin (βH) and in the hematin anhydride DMSO solvate (HA-DMSO).

Study	Intra-dimer	Inter-dimer by inversion symmetry,	Inter-dimer, by translation symmetry
Hz (present report)	9.03	7.91	8.05
Hz[a]	9.13	7.94	8.15
βH[b]	8.94	7.80	8.00
HA-DMSO[c]	8.98	5.38	-

[a]Klonis *et al.*[17], [b]Straasø *et al.*[1], [c]Gildenhuys *et al.*[18]

Figure S12: Hypothetical packing arrangement of hematin anhydride dimers assuming π- π packing similar to that in the hematin anhydride.DMSO solvate. a) H-bonded hematin anhydride dimer chains (as in Fig. 7a, main text, with its 15. 4 Å ***a-c*** axis) viewed along the H-bonding axis (as in Fig. 7b). The dimers are stacked via π-π contacts, forming a well packed layer, with an overlap of the porphyrin rings, as observed in the structure of the hematin anhydride.DMSO solvate (which has a 9.7 Å stacking axis ***a***). The latter incorporates an interdimer Fe-Fe distance of 5.38 Å (see Table S3). b) The hematin anhydride layers are juxtaposed to form a crystal with unit cell dimensions *a*=12.86 Å, *b*=10.3 Å, *c*=15.4 Å α=90.7°, β=92.7°, γ=87.7°, yielding a volume of ~2.0*10^3 Å^3, thus with volume about 40% higher than that of hemozoin.

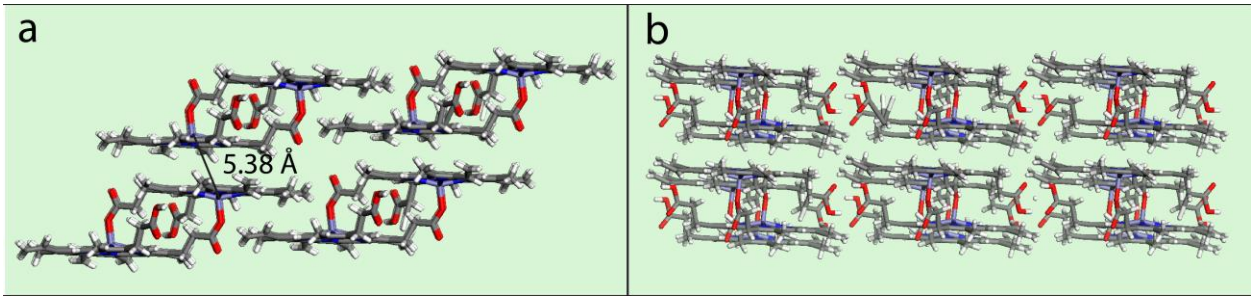

References

(1) Straasø, T.; Kapishnikov, S.; Kato, K.; Takata, M.; Als-Nielsen, J.; Leiserowitz, L. *Cryst. Growth & Des*. **2011**, *11*, 3342 (ref. 6 in main text).

(2) Vojtechovsky, J.; Chu, K.; Berendzen, J.; Sweet, R.M.; Schlichting, I. *Biophysical J.* **1999**, 77, 2153. (Ref. 17 in main text)

(3) Marom, N.; Tkatchenko, A.; Kapishnikov, S.; Kronik, L.; Leiserowitz, L. *Cryst. Growth & Des.* **2011**, *11*, 3332. (Ref. 7 in main text)

(4) Goldberg, D. E.; Slater, A. F. G.; Cerami, A.; Henderson, G. B. *P. Natl. Acad. Sci. U.S.A.* **1990**, *87*, 2931. (Ref. 50 in main text)

(5) Jackson, K. E.; Klonis, N.; Ferguson, D. J. P.; Adisa, A.; Dogovski, C.; Tilley, L. *Mol. Microbiol.* **2004**, *54*, 109. (Ref. 51 in main text)

(6) Pisciotta, J. M.; Coppens, I.; Tripathi, A. K.; Scholl, P. F.; Schuman, J.; Bajad, S.; Shulaev, V.; Sullivan, D. J. *Biochem. J.* **2007**, *402*, 197. (Ref. 52 in main text)

(7) Egan, T. J.; Chen, J. Y. J.; de Villiers, K. A.; Mabotha, T. E.; Naidoo, K. J.; Ncokazi, K. K.; Langford, S. J.; McNaughton, D.; Pandiancherri, S.; Wood, B. R. *FEBS Letters* **2006***, 580*, 5105. (Ref. 53 in main text)

(8) de Villiers, K. A.; Osipova, M.; Mabotha, T. E.; Solomonov, I.; Feldman, Y.; Kjaer, K.; Weissbuch, I.; Egan, T. J.; Leiserowitz, L. *Cryst. Growth & Des.* **2009**, *9*, 626. (Ref. 54 in main text)

(9) Wang, X.; Ingall, E.; Lai, B.; Stack, A. G. *Cryst. Growth Des.* **2010**, *10*, 798. (Ref. 55 in main text)

(10) Hoang, A. N.; Ncokazi, K. K.; de Villiers, K. A.; Wright, D. W.; Egan, T. J. *Dalton Trans.* **2010**, *39*, 1235. (Ref. 56 in main text)

(11) Kapishnikov, S.; Weiner, A.; Shimoni, E.; Guttmann, P.; Schneider, G.; Dahan-Pasternak, N.; Dzikowski, R.; Leiserowitz, L.; Elbaum, M. *P. Natl. Acad. Sci. U.S.A*. **2012**, *109*, 11188. (Ref. 57 in main text)

(12) Kapishnikov, S.; Berthing, T.; Hviid, L.; Dierolf, M.; Menzel, A.; Pfeiffer, F.; Als-Nielsen, J.; Leiserowitz, L. *P. Natl. Acad. Sci. U.S.A.* **2012**, *109*, 11184. (Ref. 58 in main text)

(13) Egan, T. J.; Mavuso, W. W.; Ncokazi, K. K. *Biochemistry-Us* **2001**, *40*, 204. (Ref. 34 in main text)

(14) Pagola, S.; Stephens, P. W.; Bohle, D. S.; Kosar, A. D.; Madsen, S. K. *Nature* **2000**, *404*, 307. (Ref. 2 in main text)

(15) Bohle, D. S.; Dinnebier, R. E.; Madsen, S. K.; Stephens, P. W. *J. Biol. Chem.* **1997**, *272*, 713. (Ref. 4 in main text)

(16) Oliveira, M. F.; Kycia, S. W.; Gomez, A.; Kosar, A. J.; Bohle, D. S.; Hempelmann, E.; Menezes, D.; Vannier-Santos, M. A.; Oliveira, P. L.; Ferreira, S. T. *FEBS Lett.* **2005**, *579*, 6010. (Ref. 5 in main text)

(17) Klonis, N.; Dilanian, R.; Hanssen, E.; Darmanin, C.; Streltsov, V.; Deed, S.; Quiney, H.; Tilley, L. *Biochemistry-Us* **2010**, *49*, 6804. (Ref. 3 in main text)

(18) Gildenhuys, J.; le Roex, T.; Egan, T. J.; de Villiers, K. A. *J. Am. Chem. Soc.* **2013**, *135*, 1037. (Ref. 11 in main text)